Spin−Spin Interactions between the Ni Site and the [4Fe-4S] Centers as a Probe of Light-Induced Structural Changes in Active *Desulfovibrio gigas* Hydrogenase[†]

François Dole,[‡] Milagros Medina,[§] Claude More,[‡] Richard Cammack,[∥] Patrick Bertrand,[‡] and Bruno Guigliarelli*,[‡]

Unité de Bioénergétique et Ingénierie des Protéines, UPR 9036, CNRS BP71, 13402 Marseille Cedex 20, France, Departamento de Bioquimica y Biologica Molecular y Celular, Universidad de Zaragoza, 50009 Zaragoza, Spain, and Division of Life Sciences, King's College, London W8 7AH, U.K.

Received July 9, 1996; Revised Manuscript Received September 30, 1996[⊗]

ABSTRACT: In typical NiFe hydrogenases like that from *Desulfovibrio gigas*, the active state of the enzyme which is obtained by incubation under hydrogen gas gives a characteristic Ni-C electron paramagnetic resonance (EPR) signal at $g = 2.19$, 2.14, and 2.01. The Ni-C species is light-sensitive, being converted upon illumination at temperatures below 100 K in a mixture of different Ni-L species, the most important giving an EPR signal at $g = 2.30$, 2.12, and 2.05. This photoprocess is considered to correspond to the dissociation of a hydrogen species initially coordinated to the Ni ion in the Ni-C state. When the [4Fe-4S] centers of the enzyme are reduced, the proximal $[4Fe\text{-}4S]^{1+}$ cluster interacts magnetically with the Ni center, which leads to complex split Ni-C or split Ni-L EPR spectra only detectable below 10 K. In order to probe the structural changes induced in the Ni center environment by the photoprocess, these spin−spin interactions were analyzed in *D. gigas* hydrogenase by simulating the split Ni-L spectra recorded at different microwave frequencies. We shown that, upon illumination, the relative arrangement of the Ni and [4Fe-4S] centers is not modified but that the exchange interaction between them is completely canceled. Moreover, the rotations undergone by the Ni center magnetic axes in the photoconversion were determined. Taken together, our results support a Ni-C structure in which the hydrogen species is not in the first coordination sphere of the Ni ion but is more likely bound to a sulfur atom of a terminal cysteine ligand of the Ni center.

Nickel−iron hydrogenases are the most commonly found enzymes that catalyze the reversible oxidation of molecular hydrogen in prokaryotic organisms (Wu & Mandrand, 1993). In the sulfate-reducing bacterium *Desulfovibrio gigas*, the enzyme has been shown to contain three iron−sulfur centers, one [3Fe-4S] and two [4Fe-4S] clusters, and a Ni center which is usually considered as the activation site of dihydrogen (Hatchikian et al., 1990; Cammack, 1992; Albracht, 1994). Several magnetic states of the Ni site have been identified by electron paramagnetic resonance (EPR) spectroscopy, depending on the redox and activation states of the enzyme (Cammack et al., 1987; Teixeira et al., 1989). Purification of the hydrogenase in the presence of air leads to an enzyme which is essentially inactive toward hydrogen and which gives a predominant EPR signal known as Ni-A ($g = 2.31$, 2.23, 2.01) and a minor signal Ni-B ($g = 2.33$, 2.16, 2.01), both signals being considered to arise from Ni-(III) species. Upon reduction, the enzyme at first becomes EPR-silent and then yields a third Ni signal, the Ni-C signal at $g = 2.19$, 2.14, and 2.01, which increases with a prolonged exposure to hydrogen gas or strong reductants and which correlates with the active form of the enzyme (Fernandez et al., 1986). Upon further reduction, the [4Fe-4S] clusters also become reduced and interact magnetically with the Ni-C species which leads to a complex spectrum detectable only below 10 K with major features at $g = 2.21$ and 2.10 (Cammack et al., 1985, 1987; Teixeira et al., 1989), and recently termed the "split Ni-C" signal (Guigliarelli et al., 1995). Finally, in the fully reduced hydrogenase, the Ni site becomes EPR-silent and only the reduced Fe-S centers are EPR-active, giving a broad and fast-relaxing signal.

In contrast with the Ni-A and Ni-B signals, which were not observed in the subclass of NiFeSe hydrogenases, the Ni-C signal was detected in all NiFe hydrogenases, showing small variations of its *g*-values in the NiFeSe enzymes (He et al., 1989; Sorgenfrei et al., 1993). The Ni-C signal is light-sensitive, being converted upon illumination at low temperature (<100 K) into a new anisotropic signal at about $g = 2.29$, 2.12, and 2.05 termed the Ni-L or Ni-C* signal (Van der Zwaan et al., 1985; Cammack et al., 1987; Asso et al., 1992; Sorgenfrei et al., 1993). The strong kinetic isotope effect observed for this photoconversion in *Chromatium vinosum* hydrogenase in D_2O led to the proposal that the Ni-C species is coordinated to a hydrogen species which dissociates upon illumination (Van der Zwaan et al., 1985). More recently, the extent of this kinetic isotope effect has been observed to vary considerably among a number of hydrogenases from different species (Medina et al., 1996). At the present time, neither the nature of the hydrogen species involved (H^+, H^-, or H_2) nor the valence state of the Ni ion [Ni(I) or Ni(III)] has been unambiguously established. The two-electron separation between the Ni-B and Ni-C states (Roberts & Lindahl, 1994), and the CO binding properties of the Ni-C species (Van der Zwaan et al., 1986; Cammack

[†] This work was supported in part by the Alliance Anglo-French joint research program 92094 and by a Biotech grant (B1 02-CT94-2041) from the European Union.

* Corresponding author.
[‡] Unité de Bioénergétique et Ingénierie des Proteines, CNRS.
[§] Universidad de Zaragoza.
[∥] King's College.

[⊗] Abstract published in *Advance ACS Abstracts,* November 15, 1996.

S0006-2960(96)01662-5 CCC: $12.00

et al., 1987) argue in favor of the Ni(I) hypothesis. In contrast, the Ni(III) assignment is supported by the similarity between the EPR properties of the Ni-L state and of oxidized Ni-substituted rubredoxins (Mus-Veteau et al., 1993; Huang et al., 1993) and by the results of some X-ray absorption experiments suggesting that the Ni ion is in the same oxidation level in the different redox forms of the enzyme (Whitehead et al., 1991; Bagyinka et al., 1993). Whether or not the Ni-C state is an intermediate of the catalytic cycle of hydrogenase is also a subject to debate, and various enzyme mechanisms have been proposed which differ essentially in the nature of the Ni-C species (Cammack et al., 1987; Hatchikian et al., 1990; Teixeira et al., 1989; Coremans et al., 1992; Huang et al., 1993; Roberts & Lindahl, 1994).

Recently, we have analyzed the magnetic interactions which develop between the nickel center and the proximal $[4Fe\text{-}4S]^{1+}$ cluster in *D. gigas* hydrogenase by simulating the split Ni-C EPR signal recorded at different microwave frequencies and by studying the relaxation enhancement of the Ni center over a wide temperature range (Guigliarelli et al., 1995). This analysis provided a detailed description of the relative arrangement of the two metal centers and gave a unifying picture of the static and dynamic effect of their magnetic coupling. In the present paper, this spin−spin coupling analysis is used to probe the structural changes induced at the Ni site upon low-temperature illumination of the Ni-C state. The EPR spectra arising from the interactions between the Ni-L and the $[4Fe\text{-}4S]^{1+}$ centers were simulated at different frequencies. The parameters deduced from these simulations demonstrate that the photoprocess is accompanied by a breaking of the exchange pathway between the two centers and allow the rotations undergone by the Ni-C magnetic axes to be specified. The implications of these results on the Ni-C structure are discussed.

MATERIALS AND METHODS

Hydrogenase from *Desulfovibrio gigas* was purified as previously described (Hatchikian et al., 1978). Samples were prepared in 50 mM 2-(*N*-morpholino)ethanesulfonate buffer, pH 6.5. The activation of the enzyme was achieved by incubation under hydrogen atmosphere at 20 °C overnight, in an electrochemical cell designed for the preparation of small-volume EPR samples (Cammack & Cooper, 1993). The redox states of the enzyme in which the nickel is in the Ni-C form and the [4Fe-4S] clusters are either oxidized or reduced were prepared as in Guigliarelli et al. (1995) by flushing the activated hydrogenase with argon till the desired potential was achieved. The redox state of the enzyme was then monitored by EPR spectroscopy.

X-band EPR spectra were recorded on a Bruker ESP300 spectrometer fitted with an Oxford Instruments ESR 900 flow cryostat. At X-band, the illumination of hydrogenase samples was carried out directly in the cryostat at the desired temperature by using a 150-W Barr & Stroud fiber optic white light through a stub waveguide fitted to the TE102 cavity. For S-band experiments, the same spectrometer was equipped with an ER061SR microwave bridge and a CF935 Oxford cryostat. In this case, illumination of samples was performed in a quartz dewar filled with liquid nitrogen, the EPR tubes being quickly transferred into the CF935 cryostat to avoid warming the samples above 100 K.

The EPR spectra arising from the spin−spin coupling between the Ni center and the proximal $[4Fe\text{-}4S]^{1+}$ cluster were simulated by using the program POINTDIP developed in our laboratory to describe the magnetic interactions between two paramagnetic point dipoles with spin $S = {}^1/_2$ (Guigliarelli et al., 1993, 1995). The main parameters used in this program are the principal values of the two **g** tensors, the spherical polar coordinates (r, θ, ϕ) which determine the position of the Ni center with respect to the [4Fe-4S] cluster, the three Euler angles (a, b, c) which define the relative orientation of the two sets of magnetic axes, and the intercenter exchange coupling constant J, defined by $H_{ex} = -2J\mathbf{S_1}\mathbf{S_2}$. In this work, the labeling of the magnetic axes (x, y, z) of the two paramagnets is defined by $g_z > g_y > g_x$.

RESULTS

Upon reduction with hydrogen gas or strong reductant, the intensity of the Ni-C EPR signal of *D. gigas* hydrogenase shows a bell-shaped variation as a function of the redox potential (Cammack et al., 1987; Teixeira et al., 1989). As the reduction of the [4Fe-4S] centers of the enzyme occurs at a slightly lower potential than the appearance of the Ni-C signal, it is possible to prepare the Ni-C form of hydrogenase in two different redox states of the enzyme, depending on the redox state of the [4Fe-4S] centers. When the [4Fe-4S] clusters are oxidized and thus diamagnetic, the enzyme gives the pure unsplit Ni-C signal with g-values at $g = 2.194$, 2.146, 2.010 (Figure 1a), whose line shape is independent of the temperature up to about 100 K. In contrast, when the [4Fe-4S] centers are reduced and thus paramagnetic, the spin−spin coupling between the Ni center and the proximal $[4Fe\text{-}4S]^{1+}$ clusters leads to a complex and fast-relaxing EPR spectrum, the split Ni-C signal (Figure 1c), only detectable at low temperature (<10 K). When the temperature is raised, the splittings of the interaction spectrum collapse progressively owing to the shortening of the $[4Fe\text{-}4S]^{1+}$ spin−lattice relaxation time, which leads to a Ni signal identical to the unsplit Ni-C signal at temperatures higher than 50 K (Guigliarelli et al., 1995).

At temperatures below 100 K, the illumination of hydrogenase samples in the unsplit Ni-C state by white light converts the Ni-C signal into a new rhombic signal previously termed Ni-C* or Ni-L. In fact, the illumination process yields a mixture of two Ni signals here referred to as Ni-L1 and Ni-L2 (Medina et al., 1996), which differ most noticeably in their highest g values, $g_z = 2.266$ and 2.296, respectively (Figure 1b). The ratio of these two species was very dependent on the temperature and on the duration of the illumination, the Ni-L1 species appearing as a transient species favored by low temperature and short duration of illumination (Medina et al., 1994). Upon illumination above 60 K, only the Ni-L2 species was obtained (Figure 2a), which allowed the Ni-L1 signal to be determined from spectral differences (Figure 3a). In the same way, when a hydrogenase sample prepared in the split Ni-C state was illuminated at low temperature, the split Ni-C signal changed into a new complex EPR spectrum only visible below 10 K (Figure 1d). At higher temperature, this complex spectrum changed into two overlapping Ni-L1 and Ni-L2 signals, so

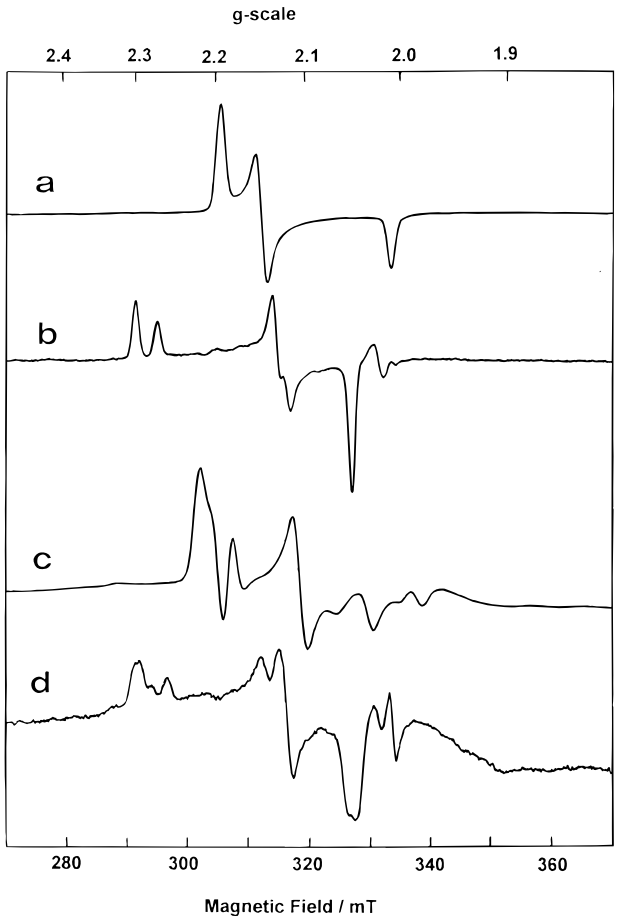

FIGURE 1: Effect of illumination on the EPR spectra of H_2-activated *D. gigas* hydrogenase. Unsplit signals given by a sample poised at −354 mV (a) before illumination and (b) after 1 min of illumination at 30 K. Split signals given by a sample poised at −376 mV (c) before illumination and (d) after 5 min of illumination at 5 K. EPR conditions: temperature (a, b) 30 K or (c, d) 5 K; microwave frequency 9.357 GHz; microwave power (a, b) 2 mW or (c, d) 0.2 mW; modulation amplitude 1 mT.

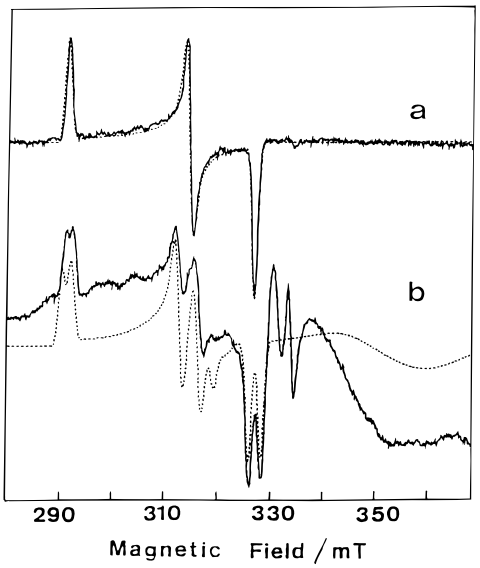

FIGURE 2: X-band EPR spectra of *D. gigas* hydrogenase in the Ni-L2 state. (a) Unsplit Ni-L2 signal given by the sample of Figure 1a after 5 min of illumination at 70 K. (b) Split Ni-L2 signal given by a sample poised at −376 mV after 15 min of illumination at 70 K. EPR conditions: temperature (a) 70 K or (b) 5 K; microwave frequency 9.356 GHz; microwave power 2 mW; modulation amplitude 1 mT. Dashed lines, numerical simulations obtained with the parameters listed in Table 1.

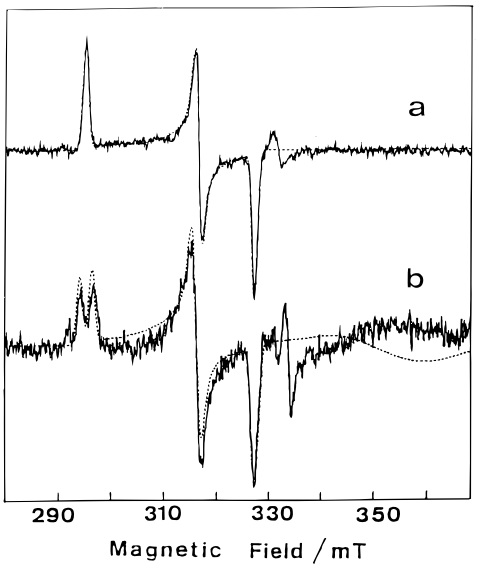

FIGURE 3: X-band EPR spectra of *D. gigas* hydrogenase in the Ni-L1 state. (a) Unsplit Ni-L1 signal obtained by subtracting the unsplit Ni-L2 signal from the spectrum of Figure 1b. (b) Split Ni-L1 signal derived by subtracting the split Ni-L2 signal from the spectrum of Figure 1d. Dashed lines, numerical simulations obtained with the parameters given in Table 1.

that it can be interpreted as arising from the magnetic interactions between the Ni-L species and the proximal fast-relaxing $[4Fe\text{-}4S]^{1+}$ cluster. The illumination of the split Ni-C state above 60 K led to a pure split Ni-L2 signal (Figure 2b), which was subtracted from the spectrum of Figure 1d to get the split Ni-L1 signal (Figure 3b).

It can clearly be seen that the splittings of the different lines exhibited by the split Ni-L2 (Figure 2b) and split Ni-L1 (Figure 3b) signals are much smaller than in the split Ni-C signal (Figure 1c), which indicates that the overall spin−spin coupling between the Ni center and the $[4Fe\text{-}4S]^{1+}$ cluster is significantly weakened by the illumination process. Moreover, although the Ni-L1 and Ni-L2 species have rather similar *g*-values (Table 1), the anisotropy of their magnetic coupling with the proximal Fe-S cluster differs significantly. The g_z line displays the smallest splitting in the split Ni-L2 signal (Figure 2b) but the largest in the split Ni-L1 one (Figure 3b). In order to interpret these observations more quantitatively, we undertook numerical simulations of both split Ni-L signals.

In a first approach, these simulations were carrried out by considering that the illumination processes only affect the coordination shell of the Ni center. The relative arrangement of the Ni and [4Fe-4S] centers was then assumed to be unchanged, and we used in this analysis the same structural parameters (r, θ, ϕ) as for the simulations of the split Ni-C signal (Guigliarelli et al., 1995). The *g*-values of the $[4Fe\text{-}4S]^{1+}$ cluster were also considered to be unaffected by the photoprocess, which was supported by the similarity of the broad signals arising from reduced Fe-S centers in the split Ni-C and split Ni-L signals (Figure 1c,d). By using for the Ni-L1 and Ni-L2 species the *g*-values deduced from the simulations of the unsplit Ni-L1 (Figure 3a) and unsplit Ni-L2 (Figure 2a) signals, good simulations of the split Ni-L1 (Figure 3b) and split Ni-L2 (Figure 2b) signals were obtained by only changing the *J* value and the orientation of the magnetic axes of the Ni center (Table 1). In a second step,

Table 1: Parameters Used for the Numerical Simulations of the EPR Signals Arising from the Spin−Spin Coupling between the Ni Center and the Proximal [4Fe-4S]$^{1+}$ Cluster[a]

	$g_{x(Ni)}$ (σ_x)[b]	$g_{y(Ni)}$ (σ_y)	$g_{z(Ni)}$ (σ_z)	J (10^{-4} cm^{-1})	(a, b, c)[c] (deg)
split Ni-C[d] signal	2.010 (5.5×10^{-3})	2.146 (5.7×10^{-3})	2.194 (5.9×10^{-3})	40	(56, 72, 105)
split Ni-L1 signal	2.045 (3.5×10^{-3})	2.115 (4.2×10^{-3})	2.265 (4.3×10^{-3})	0	(10, 35, 0)
split Ni-L2 signal	2.047 (4.0×10^{-3})	2.126 (5.5×10^{-3})	2.296 (5.5×10^{-3})	0	(80, 77, 110); (216, 97, 277)[e]

[a] The other parameters used in the simulations are $g_{x(4Fe)} = 1.860$, $g_{y(rFe)} = 1.915$, $g_{z(4Fe)} = 2.137$, $r = 0.86$ nm, $\theta = 85°$, and $\varphi = 60°$ (Guigliarelli et al., 1995). [b] Standard deviations characterizing the g-strain at X-band. [c] The accuracy on the angles is about 5°. [d] From Guigliarelli et al. (1995). [e] After refinement of the Euler angles by simulation of the S-band spectrum (see Figure 7).

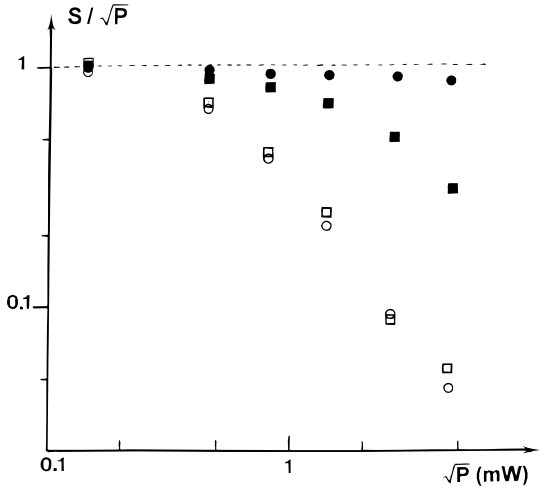

FIGURE 4: Saturation behavior of the Ni signals in activated *D. gigas* hydrogenase before and after illumination. Experimental conditions: temperature 5 K; modulation frequency 100 kHz; modulation amplitude 1 mT. Peak-to-peak amplitudes (○) of the $g = 2.146$ line of the unsplit Ni-C signal, (●) of the $g = 2.104$ line of the split Ni-C signal, (□) of the $g = 2.126$ line of the unsplit Ni-L2 signal, and (■) of the $g = 2.138$ line of the split Ni-L2 signal are shown.

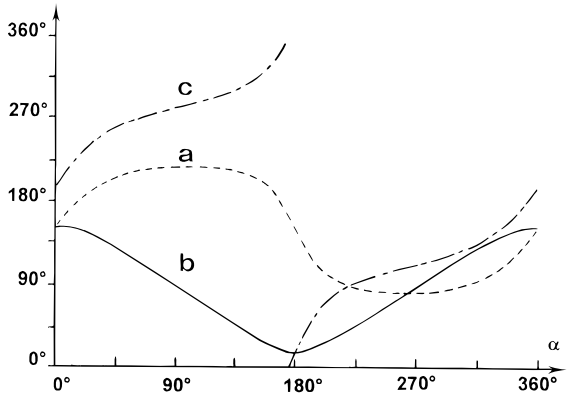

FIGURE 5: Possible values of the Euler angles (a, b, c) relating the magnetic axes of the proximal [4Fe-4S]$^{1+}$ cluster and those of the Ni-L2 species as deduced from the simulation of the split Ni-L2 signal at X-band. The angle α describes the rotation of the Ni-L2 magnetic axes about the intercenter vector **r**.

we checked that the interaction spectra calculated by changing the parameters (r, θ, φ) cannot fit the experimental split Ni-L signals. The broad signal visible on the experimental spectrum of Figure 2b likely arises from an excess of reduced [4Fe-4S] centers in the hydrogenase sample we used. Strikingly, all these simulations required a zero value for the exchange coupling constant (Table 1), and we checked that no correct simulation could be obtained by taking $|J| > 2 \times 10^{-4}$ cm^{-1}. This shows that the exchange coupling between the two metal centers is largely canceled by the illumination process.

It is well-known that at low temperature the split Ni-C signal saturates with microwave power much less easily than the unsplit Ni-C signal (Van der Zwaan et al., 1987; Teixeira et al., 1989) (Figure 4). We have shown previously that this different relaxation behavior arises from the spin−spin coupling between the Ni center and the proximal fast-relaxing [4Fe-4S]$^{1+}$ center in the split Ni-C state, and we have analyzed these differences by considering explicitly the exchange and dipolar contributions of the magnetic interaction (Guigliarelli et al., 1995). In order to make the same comparison on the light-induced signals, continuous-wave microwave power saturation experiments were performed at 5 K on the derivativelike peaks at $g = 2.126$ and $g = 2.138$ for the unsplit and split Ni-L2 signals, respectively (Figure 4). The unsplit Ni-L2 and unsplit Ni-C signals showed the same saturation behavior, indicating that the intrinsic relaxation properties of the Ni ion are not affected by illumination. Remarkably, the saturation behavior of the split Ni-L2 signal is intermediate between those of the split and unsplit Ni-C signal (Figure 4). This observation is fully consistent with the disappearance of the exchange interaction between the Ni-L2 species and the proximal [4Fe-4S]$^{1+}$ center, since in this case the relaxation enhancement of the nickel center is only due to the dipolar contribution of the magnetic coupling.

Thus, the splittings of the g_u peaks ($u = x, y, z$) observed for the split Ni-L1 and split Ni-L2 signals are only due to the dipolar interaction whose first-order contribution varies as $(1 - 3\cos^2\gamma_u)$, γ_u being the angle between the magnetic axes u of the Ni center and the interspin vector **r**. Obviously, any rotation of the Ni magnetic axes about **r** would change the Euler angles (a, b, c) while keeping the angles γ_u constant and should then lead to similar calculated spectra. Starting from the orientation of the Ni-L2 magnetic axes corresponding to the simulation of Figure 2b (Table 1), we have computed all the sets of Euler angles (a, b, c) obtained by rotating the Ni-L2 magnetic axes by an angle α about **r** (Figure 5), and we have effectively checked that any value of these sets of Euler angles led to a calculated split Ni-L2 spectrum very close to that shown in Figure 2b. Thus, it appears that the actual orientation of the Ni-L2 magnetic axes cannot be completely determined from X-band simulations only. In order to specify this actual orientation, the split Ni-L2 signal was recorded at S-band (Figure 6). The use of a lower microwave frequency enhanced the dipolar splittings relative to the **g**-tensor anisotropy, so that higher order contributions of the dipolar coupling are expected to manifest on the spectrum. Split Ni-L2 spectra were numerically calculated at S-band for each set of Euler angles defined in Figure 5 by varying the rotation angle α by 10° steps. A rotation by 180° about vector **r** led to nearly identical spectral shapes, and we observed that the α variations essentially

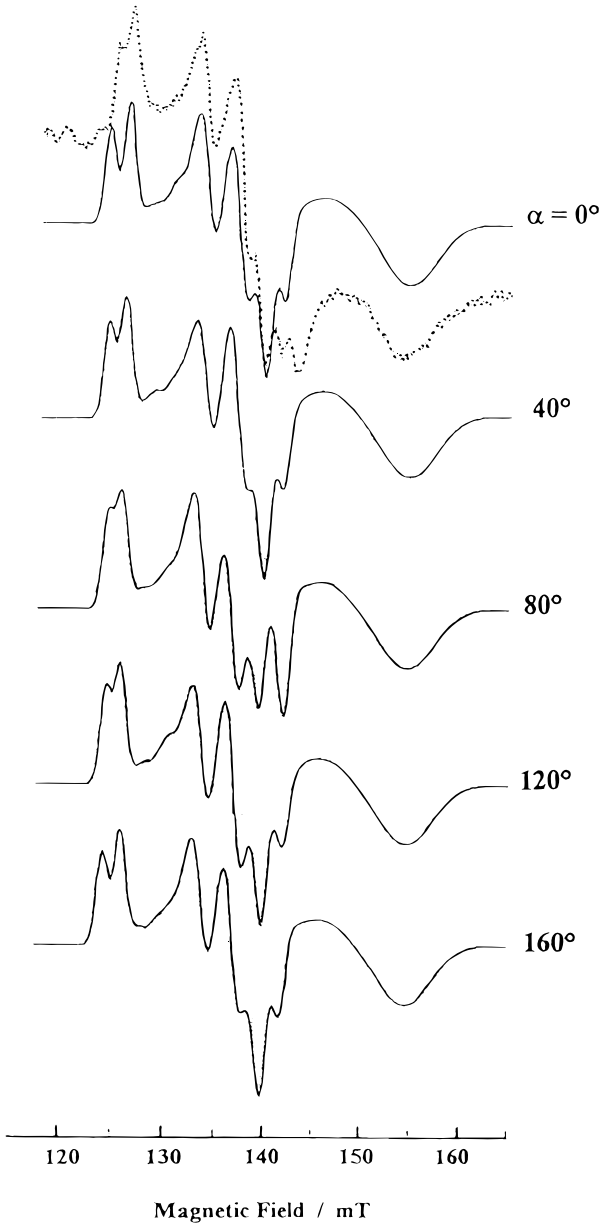

FIGURE 6: Effect of the rotation of the Ni magnetic axes about the intercenter vector **r** on the calculated split Ni-L2 spectra at S-band. The Euler angles (*a*, *b*, *c*) corresponding to the α values are deduced from Figure 5. The other parameters used in the simulations are given in Table 1. Dotted line, experimental split Ni-L2 spectrum recorded at S-band with the following conditions: temperature 5 K, microwave frequency 4.018 GHz; microwave power 0.2 mW; modulation amplitude 1 mT.

modified the relative amplitudes of the lines without significantly changing their positions (Figure 6). The comparison of the calculated spectra with the experimental one showed that only $\alpha \approx 80°$ and $\alpha \approx 260°$ led to good simulations of the S-band spectrum, the former value giving a better fit. In order to improve the split Ni-L2 signal simulations at both X-band and S-band, the Euler angles were then extensively varied around the values corresponding to these two α regions. The best simulations so obtained are given in Figure 7 and correspond to the Euler angles (*a*, *b*, *c*) = (216°, 97°, 277°). Acceptable but lesser quality fits were also obtained with (*a*, *b*, *c*) = (83°, 88°, 110°), which corresponds to $\alpha \approx 260°$. As with the Ni-L2 species, the magnetic axes of the Ni-L1 species could not be determined unambiguously from X-band simulations of the split Ni-L1

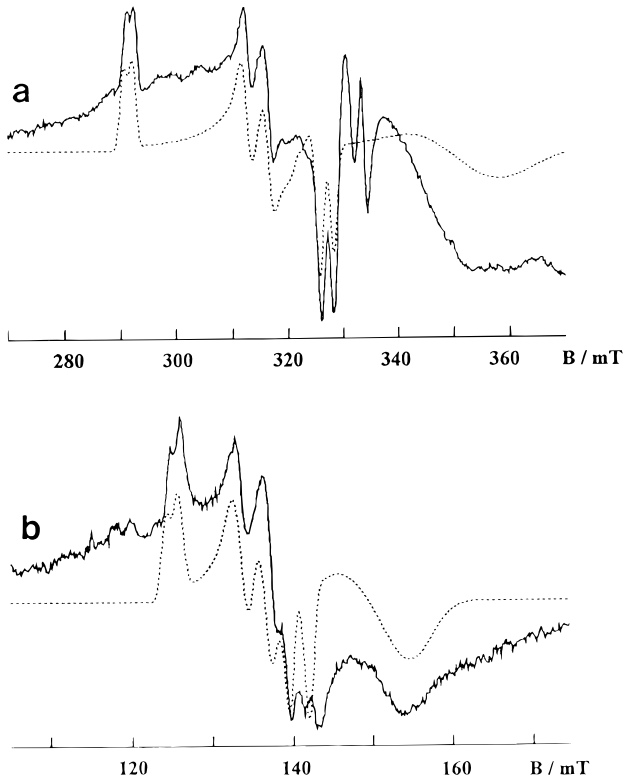

FIGURE 7: Final refinement of the numerical simulation of the split Ni-L2 signal of *D. gigas* hydrogenase. X-band (a) and S-band (b) EPR spectra. Experimental conditions as for Figure 2b (a) or Figure 6 (b). Dashed lines, numerical simulations obtained with the parameters given in Table 1.

signal only. Unfortunately, the smaller amount of the Ni-L1 species and its overlap with the Ni-L2 species precluded the S-band experiments required for a similar parameter refinement.

DISCUSSION

The light sensitivity of the Ni-C state is a general feature of all nickel hydrogenases. The finding that the rate of the photoreaction is nearly 6 times slower in D_2O than in H_2O for the *C. vinosum* hydrogenase has suggested initially that it corresponds to a breakage of a nickel−hydrogen bond (Van der Zwaan et al., 1985). Recently, the light sensitivity of the Ni-C state was studied in different nickel hydrogenases and the kinetic isotope effect observed in D_2O was found to be strongly variable, ranging from a factor of about 30 for *D. gigas* hydrogenase to about 1 for the NiFeSe enzyme from *Desulfomicrobium baculatum* (Medina et al., 1996). These results, together with the presence of at least three different paramagnetic Ni-L species generated upon illumination, indicate that the photoreaction of active hydrogenases is not a simple process and that it involves probably several rearrangements of the nickel environment, even at cryogenic temperature. The analysis of the spin−spin interactions between the Ni center and the proximal $[4Fe\text{-}4S]^{1+}$ cluster we have developed for the *D. gigas* hydrogenase (Guigliarelli et al., 1995) offers an interesting way to monitor such rearrangements by using the proximal $[4Fe\text{-}4S]^{1+}$ cluster as a magnetic probe.

The parameters deduced from the numerical simulations of the split Ni-L1 and split Ni-L2 signals (Table 1), which arise from the magnetic coupling between this FeS cluster

Table 2: Relative Orientation of the Magnetic Axes of Paramagnetic Species in Active and Illuminated *D. gigas* Hydrogenase

	solution 1	solution 2
Euler Angles between the Magnetic Axes of the Species (deg)		
$[4Fe\text{-}4S]^{1+}$ and Ni-L2	(216, 97, 277)	(83, 88, 110)
Ni-C and Ni-L2	(15, 159, 220)	(316, 31, 53)
Angle between the Magnetic Axes (deg)		
($X_{Ni\text{-}C}$, $X_{Ni\text{-}L2}$)	25	25
($Y_{Ni\text{-}C}$, $Y_{Ni\text{-}L2}$)	30	20
($Z_{Ni\text{-}C}$, $Z_{Ni\text{-}L2}$)	20	30

and the Ni-L1 or Ni-L2 species, respectively, confirmed that the illumination does not affect the relative arrangement of the two centers but modifies only the coordination sphere of the Ni center, as evidenced by the changes of its **g**-tensor. At this point, it is worth noting that in the point dipole model used in our analysis, the intercenter distance *r* is an effective parameter which differs from the center to center distance given by the crystallographic study (Volbeda et al., 1995). This study has revealed that the Ni center is actually a dinuclear Ni-X cluster in which a second metal atom X (probably iron) is located at about 0.29 nm from the Ni ion. Recently, we have improved the simulations of the split Ni-C spectrum recorded at three microwave frequencies by using a model in which the Ni center is considered as a mononuclear center and the delocalization of the spin density over the proximal $[4Fe\text{-}4S]^{1+}$ cluster is explicitly considered (Bertrand et al., 1996). The detailed arrangement of the two centers given by this model is very similar to that given by the X-ray crystal study, which supports the view that the spin density of the Ni-X center is essentially localized on the Ni site. This more detailed study confirmed the validity of the angular parameters deduced from the point dipole approach (Bertrand et al., 1996).

The numerical simulations of the split Ni-L signals performed at X-band and S-band enabled us to determine unambiguously the magnetic axes of the Ni center only for the Ni-L2 species, which is the major light-induced species. By use of the Euler angles between the magnetic axes of the $[4Fe\text{-}4S]^{1+}$ center and those of the Ni-C species, it was possible to deduce the changes induced by the photoreaction on the Ni center magnetic axes (Table 2). The angle deviations were found to be small, ranging from 20° to 30°. A similar conclusion holds for the second set of Ni-L2 magnetic directions which could not be completely excluded by considering the quality of the S-band simulations (Table 2). This shows that the magnetic axes of the Ni center in the active *D. gigas* hydrogenase are not greatly affected by the photoprocess. This result then suggests that the photochemical event does not correspond to a photolysis of a Ni−(H) bond, since in this case the removal of the (H) ligand would strongly change the coordination symmetry of the Ni ion and would induce large rotations of its magnetic axes. In particular, in the Ni-C → Ni-L2 transition, we did not observe a 90° flip of the x_{Ni} axis, the magnetic axis associated with the lowest *g* value. Such a large flip was previously proposed by Sorgenfrei et al. (1993) to interpret the influence of the illumination on the hyperfine interaction between ^{77}Se and nickel in active ^{77}Se-enriched NiFeSe hydrogenase from *Methanococcus voltae*. The discrepancy between the Sorgenfrei model and our results could be due to structural differences between the NiFe and NiFeSe hydrogenases, as suggested by the different FeS contents reported in these enzymes (He et al., 1989). However, owing to the similarity of the Ni EPR signals given by the two kinds of enzymes before and after illumination (Medina et al., 1996), a difference in the nature of the photoreaction appears rather unlikely. In fact, the analysis of the hyperfine interactions with ^{77}Se in active *M. voltae* hydrogenase was mainly based on the assumption that the Ni orbital containing the unpaired electron changes from d_{z^2} to $d_{x^2-y^2}$ upon illumination (Sorgenfrei et al., 1993). Such an analysis in terms of pure d orbitals is rigorous for ligand environments with cubic symmetry or tetragonally distorted symmetry (Loveccio et al., 1974; Jacobs & Margerum, 1984) but is no longer valid for a highly distorted Ni environment (Salerno, 1988). X-ray studies (Volbeda et al., 1995) have shown that, in oxidized *D. gigas* hydrogenase, the Ni ion is coordinated by four cysteine ligands (Cys 65, 68, 530, and 533), two of them (Cys 68 and 533) being in a bridging position between the Ni and the second metal atom X. An additional bridging oxygen atom leads to a five-coordination of the Ni ion which is very distorted. The nickel coordination is probably also distorted in the active form of the enzyme and therefore, a direct determination of the Ni magnetic axes based on the analysis of the Ni/$[4Fe\text{-}4S]^{1+}$ magnetic coupling appears to be more advisable.

When NiFe hydrogenases are prepared in D_2O, a sharpening of the Ni-C signal line widths of about 0.5 mT is observed (Van der Zwaan et al., 1985; Franco et al., 1993; Medina et al., 1996). This sharpening is consistent with the 10−20-MHz hyperfine interactions between the Ni-C species and exchangeable protons detected by electron nuclear double resonance (ENDOR) experiments in these hydrogenases (Fan et al., 1991; Whitehead et al., 1993). These weak hyperfine interactions are hardly consistent with a direct coordination of a hydrogen species to the Ni atom. Such coordination is expected to give proton hyperfine coupling of several hundred megahertz (Symons et al., 1979), which would lead to a splitting or to a strong broadening of the Ni-C EPR lines. Furthermore, in the case of NiFeSe enzymes, no linewidth difference was detected for the Ni-C signal in D_2O as compared with H_2O (Sorgenfrei et al., 1993; Medina et al., 1996). This result is consistent with the absence of kinetic isotope effect in D_2O on the Ni-C to Ni-L conversion in NiFeSe hydrogenases (Medina et al., 1996). All these observations, together with our finding that the magnetic axes of the Ni-C and Ni-L2 species are very close, thus suggest that the hydrogen (H) species, which is believed to be removed upon illumination, is not in the first coordination sphere of the Ni ion. Instead, this (H) species could be bound either to a ligand of the Ni atom or to the second metal atom X of the Ni-X cluster. Owing to their bridging position, the thiolate ligands from Cys 68 and Cys 533 are likely excluded. The metal ion X can also be ruled out since our recent results indicate that it is diamagnetic in the Ni-C state (Bertrand et al., 1996; Dole, Guigliarelli, and Bertrand, unpublished results) and cannot mediate hyperfine interactions with a (H) species. Thus, good candidates for the binding of the (H) species could be either the μ-oxo ligand, if this atom is still present in the active hydrogenase, or one of the terminal sulfur ligands of the Ni ion (Cys 65 or Cys 530). We favor this last proposal, which is in agreement with the structural model proposed by Roberts and Lindahl (1994) for the Ni-C species on the basis of detailed redox titrations of *D. gigas*

hydrogenase. In particular, the binding of the (H) species to Cys 530, which is equivalent to the selenocysteine of NiFeSe hydrogenases, could explain the different properties of the NiFe and NiFeSe enzyme regarding the proton hyperfine interactions in the Ni-C state, the kinetic isotope effect of the Ni-C → Ni-L photoconversion, and possibly the catalytic activity (Teixeira et al., 1987).

A striking phenomenon occurring upon illumination of active *D. gigas* hydrogenase is the complete cancellation of the exchange interaction between the Ni center and the proximal $[4Fe\text{-}4S]^{1+}$ cluster (Table 1). This occurs even in the first step of the photoprocess since a zero value of the *J* constant was found to be required for simulating the split Ni-L1 signal. Before illumination, the magnitude of the exchange interaction between the Ni-C species and the $[4Fe\text{-}4S]^{1+}$ center (Table 1) is comparable to those found between the two $[4Fe\text{-}4S]^{1+}$ clusters of reduced bacterial ferredoxins (More et al., 1996), the intercenter distance being close to 1.2 nm in both systems. However, it is important to note that, in these ferredoxins, the two [4Fe-4S] centers are carried by the same polypeptide chain, whereas the Ni center and the FeS clusters of hydrogenase are coordinated by two different subunits (Volbeda et al., 1995). The exchange interaction between two paramagnetic centers arises from the residual overlap of magnetic orbitals through chemical bonds involving the intercenter medium (Bencini & Gatteschi, 1990). Therefore, the disappearance of the exchange coupling between the Ni center and the $[4Fe\text{-}4S]^{1+}$ cluster after illumination might be explained if the (H) species is involved in a bond pathway connecting these two centers and then the two subunits α and β. This hypothesis is consistent with the binding of the (H) species to one of the terminal thiolate ligands of the Ni ion (Cys 65 and Cys 530), which point toward the proximal [4Fe-4S] cluster, and the exchange pathway connecting the Ni and [4Fe-4S] centers in active hydrogenase could be involved in the electron transfer mechanism. Upon illumination at low temperature, the bond between the (H) species and the thiolate ligand would be broken, which would change the Ni-C EPR species into Ni-L species and would suppress the exchange interaction between the Ni center and the proximal [4Fe-4S] cluster. Since the Ni-C signal is simply restored by warming the enzyme above about 100 K, the photodissociated (H) species likely stays close to the Ni metal center, as the CO molecule behaves upon irradiation of CO-myoglobin (Frauenfelder, 1979). The presence of several Ni-L species could be related to different locations of the photodissociated (H) species and/or to different conformations of the Ni environment. Alternatively, the presence of two different (H) species bound to Cys65 and Cys530, respectively, as suggested by the Ni-C model of Roberts and Lindahl (1994), cannot be excluded, and their successive removal could explain the existence of three Ni-L species.

This model then suggests that the binding sites of the (H) species and of the carbon monoxide, which is a competitive inhibitor of dihydrogen (Hallahan et al., 1986), are different. The binding of CO to active NiFe hydrogenases has been observed in a number of species and leads to the conversion of the Ni-C signal into a Ni-CO signal (Van der Zwaan et al., 1986; Cammack et al., 1987). By use of ^{13}CO, a strong hyperfine splitting of the Ni-CO signal was observed and was interpreted as arising from the direct binding of the CO molecule to the Ni ion (Van der Zwaan et al., 1990). The analysis of the magnetic interactions between the Ni-CO species and the proximal $[4Fe\text{-}4S]^{1+}$ cluster would be useful to specify the location of the CO molecule in the Ni active site, and experiments are in progress with this aim.

REFERENCES

Albracht, S. P. J. (1994) *Biochim. Biophys. Acta 1188*, 167−204.

Asso, M., Guigliarelli, B., Yagi, T., & Bertrand, P. (1992) *Biochim. Biophys. Acta 1122*, 50−56.

Bagyinka, C., Whitehead, J. P., & Maroney, M. J. (1993) *J. Am. Chem. Soc. 115*, 3576−3585.

Bertrand, P., Camensuli, P., More, C., & Guigliarelli, B. (1996) *J. Am. Chem. Soc. 118*, 1426−1434.

Cammack, R. (1992) Catalysis by Nickel in Biological Systems, in *Bioinorganic Chemistry* (Reedijk, J., Ed.) Marcel Dekker, New York.

Cammack, R., & Cooper, C. E. (1993) EPR Spectroscopy of Iron Complexes and Iron-Containing Proteins, in *Methods in Enzymology, Metallobiochemistry, Part C* (Riordan, J. & Vallee, B., Eds.) Vol. 227, pp 353−384, Academic Press, San Diego, CA.

Cammack, R., Patil, D. S., & Fernandez, V. M. (1985) *Biochem. Soc. Trans. 13*, 572−578.

Cammack, R., Patil, D. S., Hatchikian, E. C., & Fernandez, V. M. (1987) *Biochim. Biophys. Acta 912*, 98−109.

Coremans, J. M. C. C., Van der Zwaan, J. W., & Albracht, S. P. J. (1992) *Biochim. Biophys. Acta 1119*, 157−168.

Fan, C., Teixeira, M., Moura, J., Moura, I., Huynh, B. H., LeGall, J., Peck, H. D., & Hoffman, B. M. (1991) *J. Am. Chem. 113*, 20−24.

Fernandez, V. M., Hatchikian, E. C., Patil, D., & Cammack, R. (1986) *Biochim. Biophys. Acta 883*, 145−154.

Franco, R., Moura, I., LeGall, J., Peck, H. D., Huynh, B. H., & Moura, J. J. G. (1993) *Biochim. Biophys. Acta 1144*, 302−308.

Frauenfelder, H. (1979) in *Tunneling in Biological Systems* (Chance, B., Don DeVault, C., Frauenfelder, H., Marcus, R. A., Schrieffer, J. R., & Sutin, N., Eds.) pp 627−649, Academic Press, New York.

Guigliarelli, B., Guillaussier, J., More, C., Setif, P., Bottin, H., & Bertrand, P. (1993) *J. Biol. Chem. 268*, 900−908.

Guigliarelli, B., More, C., Fournel, A., Asso, M., Hatchikian, E. C., Williams, R., Cammack, R., & Bertrand, P. (1995) *Biochemistry 34*, 4781−4790.

Hallahan, D. L., Fernandez, V. M., Hatchikian, E. C., & Hall, D. O. (1986) *Biochimie 68*, 49−54.

Hatchikian, E. C., Bruschi, M. & LeGall, J. (1982) *Biochem. Biophys. Res. Commun. 82*, 451−461.

Hatchikian, E. C., Fernandez, V. M., & Cammack, R. (1990) *FEMS Symp. 54*, 53−73.

He, S. H., Teixeira, M., LeGall, J., Patil, D. S., Moura, I., Moura, J. J. G., DerVartanian, D. V., Huynh, B. H., & Peck, H. D. (1989) *J. Biol. Chem. 264*, 2678−2682.

Huang, Y. H., Park, J. B., Adams, M. W. W., & Johnson, M. K. (1993) *Inorg. Chem. 32*, 375−376.

Jacobs, S. A., & Margerum, D. W. (1984) *Inorg. Chem. 23*, 1195−1201.

Medina, M., Williams, R., Cammack, R., & Hatchikian, E. C. (1994) *J. Chem. Soc., Faraday Trans. 90*, 2921−2924.

Medina, M., Hatchikian, E. C., & Cammack, R. (1996) *Biochim. Biophys. Acta 1275*, 227−236.

More, C., Camensuli, P., Dole, F., Guigliarelli, B., Asso, M., Fournel, A., & Bertrand, P. (1996) *J. Biol. Inorg. Chem. 1*, 152−161.

Mus-Veteau, I., Diaz, D., Gracia-Mora, J., Guigliarelli, B., Chottard, G., & Bruschi, M. (1991) *Biochim. Biophys. Acta 1060*, 159−165.

Roberts, L. M., & Lindahl, P. A. (1994) *Biochemistry 33*, 14339−14350.

Salerno, J. C. (1988) in *The Bioinorganic Chemistry of Nickel* (Lancaster, J. R., Ed.) pp 53−73, VCH Publishers, New York.

Sorgenfrei, O., Klein, A., & Albracht, S. P. J. (1993) *FEBS Lett. 322*, 291−297.

Symons, M. C. R., Aly, M. M., & West, D. X. (1979) *J. Chem. Soc., Chem. Commun.*, 51−52.

Teixeira, M., Fauque, G., Moura, I., Lespinat, P. A., Berlier, Y., Pickrill, B., Peck, H. D., Xavier, A. V., LeGall, J., & Moura, J. J. G. (1987) *Eur. J. Biochem. 167*, 47−58.

Teixeira, M., Moura, I., Xavier, A. V., Moura, J. J. G., LeGall, J., DerVartanian, D., Peck, H. D., & Huynh, B. H. (1989) *J. Biol. Chem. 264*, 16435−16450.

Van der Zwaan, J. W., Albracht, S. P. J., Fontijn, R. D., & Slater, E. C. (1985) *FEBS Lett. 179*, 271−277.

Van der Zwaan, J. W., Albracht, S. P. J., Fontijn, R. D., & Roelofs, Y. B. M. (1986) *Biochim. Biophys. Acta 872*, 208−215.

Van der Zwaan, J. W., Albracht, S. P. J., Fontijn, R. D., & Mul, P. (1987) *Eur. J. Biochem. 169*, 377−384.

Van der Zwaan, J. W., Coremans, J. M. C. C., Bouwens, E. M. C., & Albracht, S. P. J. (1990) *Biochim. Biophys. Acta 1041*, 101−110.

Volbeda, A., Charon, M. H., Piras, C., Hatchikian, E. C., Frey, M., & Fontecilla-Camps, J. (1995) *Nature 373*, 580−587.

Whitehead, J. P., Colpas, G. J., Bagyinka, C., & Maroney, M. J. (1991) *J. Am. Chem. Soc. 113*, 6288−6289.

Whitehead, J. P., Gurbiel, R. J., Bagyinka, C., Hoffman, B. M., & Maroney, M. J. (1993) *J. Am. Chem. Soc. 115*, 5629−5635.

Wu, L. F., & Mandrand, M. A. (1993) *FEMS Microbiol. Rev. 104*, 243−270.

BI961662X